pISSN:2093-274x eISSN:2093-2480
DOI:10.5139/IJASS.2010.11.1.049

Shock Response Prediction of a Low Altitude Earth Observation Satellite During Launch Vehicle Separation

Dae-Oen Lee* and Jae-Hung Han**
Department of Aerospace Engineering
Korea Advanced Institute of Science and Technology, Daejeon, 350-701, Korea

Hae-Won Jang***
Department of Mechanical Engineering
Korea Advanced Institute of Science and Technology, Daejeon, 350-701, Korea

Sung-Hyun Woo** and Kyung-Won Kim******
Korea Aerospace Research Institute, Daejeon, 350-333, Korea

Abstract

Several pyrotechnic devices are employed over the course of satellite's missions, generally for the separation of structural subsystems and deployment of appendages. Firing of pyrotechnic devices results in impulsive loads characterized by high peak acceleration and high frequency content which can cause failures of various flight hardware elements and small components. Thus, accurate prediction of acceleration level in various components of spacecraft due to pyrotechnic devices is important. In this paper, two methods for pyroshock prediction, an empirical model and statistical energy analysis in conjunction with virtual mode synthesis, are applied to predict shock response of a low altitude earth observation satellite during launch vehicle separation. The predicted results are then evaluated through comparison with the shock test results.

Key Words : Pyroshock, Shock Response Spectrum, Statistical Energy Analysis, Virtual Mode Synthesis and Simulation

Introduction

Several pyrotechnic devices containing high explosives are employed over the course of satellite' s missions, generally for the separation of structural subsystems and deployment of appendages. Firing of pyrotechnic devices results in impulsive loads characterized by high peak acceleration, high frequency content and short duration, and the resulting transient response of structural systems and subsystems is called pyrotechnic shock or pyroshock [1].

* M.S. Candidate
** Professor
E-mail : jaehunghan@kaist.ac.kr
Tel : +82-42-350-3723 Fax : +82-42-350-3710
*** Ph. D Candidate
**** Researcher

The complexity of the waveform and extremely short duration of a pyroshock make it impossible to define a unique explicit description of the environment for test specification purposes. Furthermore, reproduction of exact pyroshock for testing is practically impossible [2]. The accepted standard for implicit description is the shock response spectrum (SRS) which is a useful tool for estimating damage potential of the shock pulse and for test level specification. SRS is computed using an acceleration time history of the actual environment which is applied as an excitation to a hypothetical base on which single degree of freedom (SDOF) systems are attached via spring and dashpot. The damping of all SDOF system are usually assumed to be 5% (Q=10), while the natural frequency of each SDOF system is chosen to be different. The SRS is defined as the largest peak absolute acceleration response

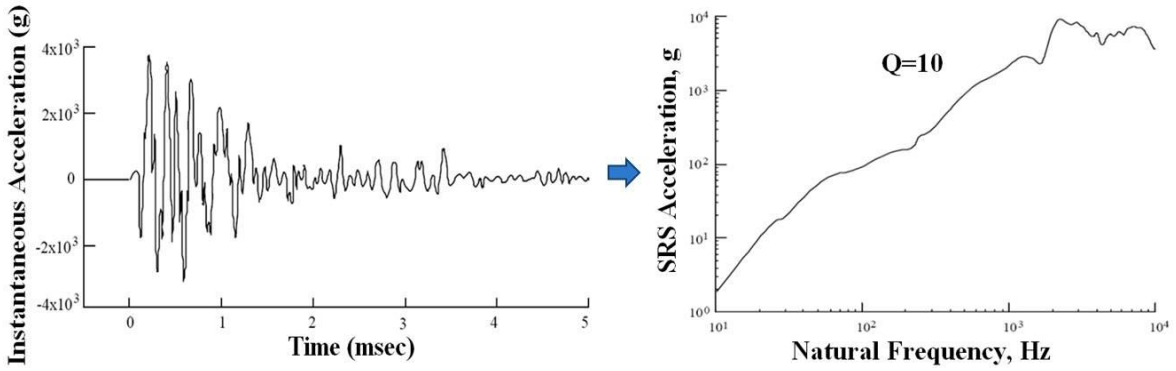

Fig. 1. Typical pyroshock time history and its corresponding SRS [1]

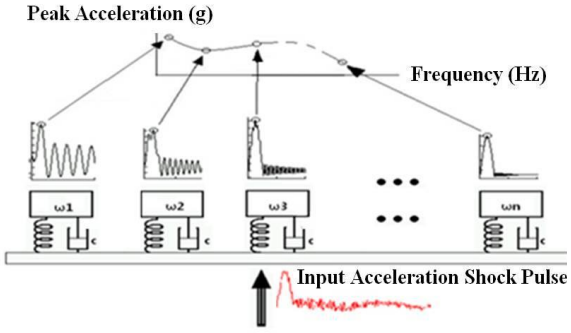

Fig. 2. The concept of SRS

of each SDOF system to the time history base input plotted against the natural frequency of SDOF systems [3]. Fig. 1 shows a typical pyroshock acceleration time history and its corresponding SRS. Fig. 2 illustrates the concept of SRS.

Due to the high frequency and short duration character of the loads, the damages caused by the activation of pyrotechnic devices are essentially confined to the parts of payload that have very high frequency resonances including many electronic devices and small components. Specifically, cracks and fractures in crystals, ceramics, epoxies and solder joints, relay and switch chatter and transfer, failures in circuit boards and computer memory, etc are attributed to pyroshock exposure. These failures may result in catastrophic mission loss [1]. Therefore, accurate prediction of acceleration levels due to pyrotechnic devices is desirable in the preliminary design phase for the definition of payload shock environment to guarantee the operation of shock sensitive parts.

However, prediction of acceleration levels due to the operation of pyrotechnic devices is a very complicated task as the high frequency character of pyroshock makes prediction of structural responses using classical normal mode analysis and finite element methods ineffective. Alternative methods used to predict the response of space vehicle structures to pyrotechnics loads and their merits are listed in table 1, but experimental pyroshock verification almost always accompanies the predictions due to the limitations in the prediction accuracy.

In Korea, shock environment resulting from the activation of pyrotechnic devices used in satellites is measured using a structure and thermal model (STM) of the satellites through pyroshock tests in the later design phase, and pyroshock prediction is usually ignored. Although these tests provide valuable information, some a priori knowledge on the expected shock environment in the preliminary design phase are very much desired. The procedures listed in table 1 are believed to offer the best approaches for preliminary design purposes, and for the final design, direct measurement techniques, perhaps supported by statistical energy analysis procedures, will usually produce more accurate results [4].

In this paper, two methods applicable for pyroshock prediction, an empirical model and statistical energy analysis (SEA) in conjunction with virtual mode synthesis and simulation (VMSS) are applied to predict launch vehicle separation shock response of a low altitude earth observation satellite. For prediction verification, the predicted shock levels are compared and examined using the data obtained during launch vehicle separation test on the STM of the low altitude earth observation satellite.

Table 1. The merits of various high frequency transient response prediction procedures [4]

Merit	Analytical	Empirical	Transient SEA and VMSS	Extrapolation
Relatively easy to accomplish	No	Yes	No	Yes
Applicable in preliminary design	No	Yes	Yes	Yes
Applicable before first launch	Yes	Yes	Yes	Yes
Applicable to radical new vehicle design	Yes	No	Yes	No

Launch Vehicle Separation Test

Launch vehicle separation test was conducted on the STM of the low altitude earth observation satellite by researchers at KARI to verify the shock test level for the qualification and acceptance on the spacecraft (S/C) during the ignition of the launch vehicle (L/V) separation system and to perform the mechanical fit check. For the satellite under consideration, total of six pyros are installed between S/C adapter and L/V simulator. Fig. 3 shows location of pyros. Activation of pyros are divided into two parts where the first three pyros (+X+Y, −X+Y, −Y, i.e. pyros marked in red circle on Fig. 3) are simultaneously activated which is promptly followed by firing of the remaining three pyros (+Y, +X−Y, −X−Y, i.e. pyros marked in black square on Fig. 3). Launch vehicle separation test was performed twice and the test results were recorded in SRS based on 1/12 octave bands from 100 Hz ~ 10 kHz. Only the maximum values of the two tests are used for comparison with the prediction results.

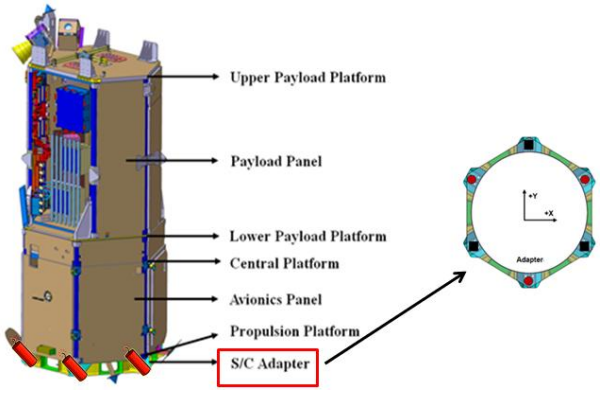

Fig. 3. Location of pyros for launch vehicle separation

Empirical Model

Empirical model used for pyroshock prediction is based on the observed characteristics of pyroshock from the accumulated test data. Empirical model predicts expected shock levels using SRS based on the types of pyrotechnic source and the attenuation of shock levels as a function of distance from the source and due to the joints connecting substructures. Empirical model is relatively easy to accomplish and can be applied without the need for detailed information of the structure, making it a useful tool in preliminary design phase [4]. Although the results are empirical and based on a limited amount of data, insight into the characteristics of SRS produced by various sources as well as the attenuation of the shock through various structural elements can be obtained. In this section, methods for assessing expected shock levels using empirical model is summarized.

In order to apply empirical model, the SRS of shock source must be divided into low and high frequency region as shock attenuation characteristics in each frequency region are observed to differ. Typical SRS of pyrotechnic

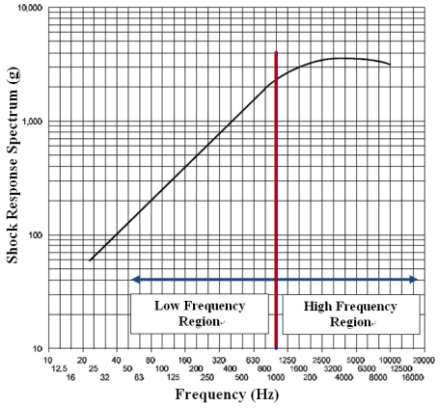

Fig. 4. Distinction of low and high frequency region in typical SRS of pyrotechnic device

devices exhibits constantly increasing curve at low frequencies and steady or decreasing curve at high frequencies after reaching the peak level, and the SRS can be divided accordingly into a low and high frequency region as shown in Fig. 4.

A pyroshock environment is more realistically characterized as a traveling wave response phenomenon than a classical standing wave response of vibration modes. This nature of shock causes rapid attenuation of shock level as a function of distance from the source and as it crosses structural discontinuities produced by joints and interfaces [3].

Shock attenuation with distance from the source

Shock is attenuated as a function of distance from the source. Observations of the accumulated pyroshock data show that shock attenuation due to distance is independent of structure's type in low frequency region (Fig. 5.a) while at high frequencies it becomes a function of distance as well as structure type (Fig. 5.b) [3]. Note that the distance from the source is given in inches in Fig. 5.

Shock attenuation due to discontinuities

In addition to gradual attenuation of shock as a function of distance, shock levels are abruptly attenuated when the response wave traverses discontinuities produced by joints and interfaces [3]. Shock attenuation due to a joint is very complex phenomenon and it is almost impossible to assign a specific value even for the same type of joints and interfaces as it tends to vary greatly. Guideline levels of reduction for some common interfaces are suggested in [3] but only at a very crude level. [4] recommends the estimated shock attenuation of SRS due to joint to be 40% per joint up to a maximum of three joints for the peak SRS value, i.e. high frequency region, and no attenuation in the low frequency region. Good engineering sense is required to choose an appropriate attenuation value for each discontinuity, and more studies are needed for better shock attenuation estimates due to joints and interfaces.

Launch vehicle separation shock prediction using empirical method

In order to estimate expected shock levels in various parts of the satellite using the empirical model described above, knowledge of the location and the SRS of the shock source and structural information of the satellite is required. Obtaining SRS that best represents the SRS of the real shock source is especially important as shock response of every other part of the satellite is derived from it. SRS for various point source pyrotechnic devices can be found in [4], but for the satellite in consideration, SRS of the shock source is provided by the manufacturer of the pyrotechnic device used in the launch vehicle separation test (table 2). Better estimate of shock level is expected by taking SRS provided by the manufacturer than using a representative SRS given in [4].

The required structural information of the satellite for the empirical model are the distance of response location from the shock source (listed in table 3), the structure type of the shock path identified as one of the categories of structure given in Fig. 4.b and the number of discontinuities in the shock path from the shock source to the substructure of interest (also listed in table 3). The pyros are installed between S/C adapter and L/V simulator, so the shock source is located on S/C adapter. It is assumed that the shock induced by the activation of pyros installed on S/C adapter is transmitted directly to propulsion platform and avionics panel, and indirectly to other substructures through longeron. In this paper, shock attenuation due to joint suggested by [4] is adopted so that each joint is assumed to attenuate 40% of the shock in the high frequency region and none in the low frequency region.

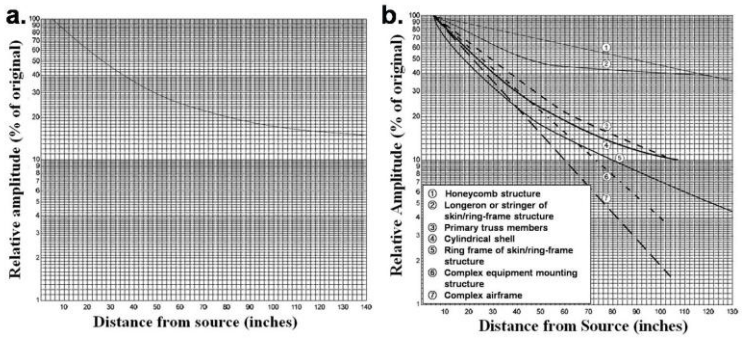

Fig. 5. Shock attenuation due to distance in low and high frequency region [3]

Table 2. SRS level of the shock source

Frequency	SRS (g)
100	70
1500	3000
10000	3000

Table 3. Structural information of the satellite

Substructure	Distance (inch)	Number of joints
Propulsion Platform	5.5	1
Central Platform	5.5+41	1
Lower Payload Platform	5.5+52	2
Upper Payload Platform	5.5+52+68	3
Avionics Panel	5.5	1
Payload Panel	5.5+52	2

Shock prediction using the empirical model can be performed readily once the distance from the shock source and type of structure and number of discontinuities in the shock path is identified. The distance between the S/C adapter and the propulsion module is 5.5 inches and the shock path is through the adapter which can be seen as cylindrical shell. From Fig. 4, this corresponds to no shock attenuation due to distance in both low and high frequency region. There is one joint in between which attenuates 40% of shock source in high frequency region and none in low frequency region. Thus, there is no shock attenuation at low frequency region but 40% reduction at high frequency region in total for propulsion platform and avionics panels. The attenuated shock is transmitted to other parts of the satellite through longeron. Following a similar procedure, the expected shock levels for other components can be calculated. The only difference is that when the shock traverses a joint, the attenuated shock becomes a new shock source and the distance to other subsystems is calculated accordingly. For example, central platform is located 46.5 inches away from the shock source but the shock path includes one joint at 5.5 inches from the shock source. Thus, attenuated shock is calculated for the first 5.5 inch which becomes a new shock source. Then, shock attenuation due to the remaining distance of 41 inches, 65% in low frequency region and 48% in high frequency region, is calculated using the new shock source. Thus, only 35% and 32.2% (0.6*0.52) of the original shock is predicted at central platform in low and high frequency region respectively. The shock prediction results using the described empirical model is given with the prediction results using SEA and VMSS (Figs. 6a~6g) for comparison after the discussion of shock prediction using SEA and VMSS.

Virtual Mode Synthesis and Simulation

SEA [5] is the most widely used and established vibration analysis method at high frequencies. In SEA, complex structure is divided into coupled subsystems that can store, transmit and dissipate energy, and the dynamic system response levels are predicted using steady state power balance equations. Although the use of steady state power balance equations allows great simplification in terms of mathematics, it limits the application of SEA to steady state response predictions. However, the band averaged frequency response function (FRF) magnitude obtained from SEA can be used in conjunction with VMSS [6] to accomplish transient response prediction. The fundamental assumption of VMSS is that at high frequencies

where large number of modes exists, the frequency response envelope can be represented as the peak response from a collection of localized vibration modes with frequencies spaced according to the estimated modal density of the local structure. Virtual modes can be roughly defined as approximations of the actual physical modes which produce FRF mapping to the desired FRF and the result of virtual mode synthesis process is a vector containing approximations to the mode shape coefficient products for the i^{th} response and j^{th} force at each virtual mode frequency [7]. The normal mode equations used by VMSS are of the form,

$$[M]\{\ddot{\xi}\} + [D]\{\dot{\xi}\} + [K]\{\xi\} = [\Phi]^T\{F(t)\} \quad (1)$$

where $[M]$, $[D]$, $[K]$, $[\Phi]^T$ are generalized mass, damping, stiffness and virtual mode shape matrices respectively, and $\{F(t)\}$ and $\{\xi\}$ are vectors for applied loads and the modal coordinate respectively. Under light damping approximation, the frequency response magnitude becomes a summation of the magnitude of each mode response as

$$\left|H_{ij}(\Omega)\right| = \left|\frac{q_i(i\Omega)}{F_j(i\Omega)}\right| = \sum_{m=1}^{n_m} \frac{\phi_{im}\phi_{jm}}{\sqrt{(\omega_m^2 - \Omega^2)^2 + (2\zeta_m\omega_m\Omega)^2}} \quad (2)$$

where n_m is the number of modes in the substructure selected for response. For convenience, this FRF magnitude can be rewritten as the product of two vectors,

$$\left|H_{ij}(\Omega)\right| = \{\Lambda\}^T\{\Phi\}_{ij} \quad (3)$$

where

$$\{\Lambda\} = \left\{ \begin{array}{c} \frac{1}{\sqrt{(\omega_1^2-\Omega^2)^2+(2\zeta_1\omega_1\Omega)^2}} \\ \frac{1}{\sqrt{(\omega_2^2-\Omega^2)^2+(2\zeta_2\omega_2\Omega)^2}} \\ \vdots \\ \frac{1}{\sqrt{(\omega_{n_m}^2-\Omega^2)^2+(2\zeta_{n_m}\omega_{n_m}\Omega)^2}} \end{array} \right\} \text{ and } \{\Phi\}_{ij} = \left\{ \begin{array}{c} \phi_{i1}\phi_{j1} \\ \phi_{i2}\phi_{j2} \\ \vdots \\ \phi_{in_m}\phi_{jn_m} \end{array} \right\} \quad (4)$$

By packing the FRF magnitudes available from steady state methods into a column vector $\{|H|\}$, where each element of the vector represents the FRF magnitude at the assumed virtual mode frequencies, the synthesis operation for virtual modes can be performed. Equating the column vector elements to equation 4 results in

$$\{\left|H(\Omega)\right|\}_{ij} = [\Lambda]^T\{\Phi\}_{ij} \quad (5)$$

where

$$[\Lambda] = [\{\Lambda(\Omega_1)\} \quad \{\Lambda(\Omega_2)\} \quad \cdots \quad \{\Lambda(\Omega_{n_m})\}] \quad (6)$$

The virtual mode coefficients are then obtained from the relationship

$$\{\Phi\}_{ij} = ([\Lambda]^T)^{-1}\{\left|H\right|\}_{ij} \quad (7)$$

Since the FRF envelope is produced at resonant frequencies of the virtual modes, $\{\left|H(\Omega)\right|\}$ is evaluated at those frequencies, which are populated across the bandwidth according to the modal density of the response substructure. With the synthesized virtual mode coefficients, the governing equation 1 can be solved for time response and SRS may be obtained.

Launch vehicle separation shock prediction using SEA and VMSS

In this section, SEA and VMSS are used to predict shock response of the low altitude earth observation satellite during launch vehicle separation. SEA model provides frequency band averaged FRFs necessary for the synthesis of virtual modes. In addition damping loss factors and modal densities from SEA model can be adapted in VMSS. In this paper, commercial software VA One 2007 is used to construct SEA model and perform shock analysis. In VA One 2007, modal parameters (modal density and damping loss factors) are automatically adapted from the SEA model. The number of modes to be synthesized is determined by the modal density of a subsystem selected for response and the synthesized modes are evenly spaced across a frequency band. One drawback of the software is that it can only manage one input force defined by its time history. In aerospace industry, pyroshocks are usually defined by SRS. Thus, it is necessary to find a force time history that will result in the desired SRS. For this force tuning work, force time history in the form of half sine wave was used to find SRS that best resembles the measured SRS at the propulsion platform which is the nearest substructure from the shock source. The determined force time history was then used as the shock source for response predictions in other parts of the satellite.

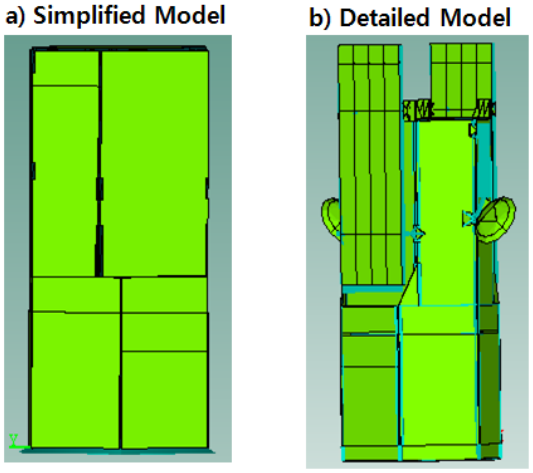

Fig. 5. Simplified and detailed SEA model used for shock analysis

Various SEA models are examined to find the SEA model that gives best estimates to the test results. Due to the difficulties involved in exciting structures in the frequency range of interest (100 Hz ~ 10 kHz) involving high frequencies, experimental determination of the loss factors is omitted. Instead SEA models with various assumed damping loss factors are examined (equation 8a~8.c). Comparison with the experimental results shows that prediction results with the damping model described by equation 8.a are closest to the experimental ones in most parts of the satellite.

$$\eta = \begin{cases} 0.05 & f \le 500\ \text{Hz} \\ 0.05 \times 500/f & f > 500\ \text{Hz} \end{cases} \quad (8.a)$$

$$\eta = \begin{cases} 0.01 & f \le 100\ \text{Hz} \\ 0.01 \times 100/f & f > 100\ \text{Hz} \end{cases} \quad (8.b)$$

$$\eta = 0.01 \quad \text{for all frequency range} \quad (8.c)$$

Also, shock analysis using simplified and detailed SEA model is performed. In the simplified model, subsystems with low modal densities and other components of the satellite that are weakly connected to the main body are omitted while these components are included in the detailed model (Fig. 5). For both models, damping model described by equation 8.a is used.

Shock Prediction Results and Discussions

In this section, shock response prediction results of the low altitude earth observation satellite during launch vehicle separation is summarized and discussed. Figs. 6a~6g shows the comparison of prediction results obtained using empirical model and SEA and VMSS with the test results.

The predicted shock levels using the empirical model provide good envelop for the test results in most of the frequency ranges except at very high frequencies. In general, the prediction results obtained through the empirical model tends to somewhat overestimate response in low frequency region while underestimating response in higher frequency region. This may be partly remedied by altering shock attenuation caused by joints. Considering the effort exerted in obtaining these prediction results, the accuracy of the returned results are quite satisfactory.

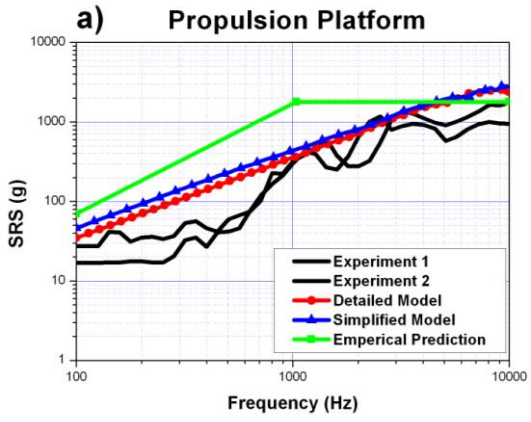

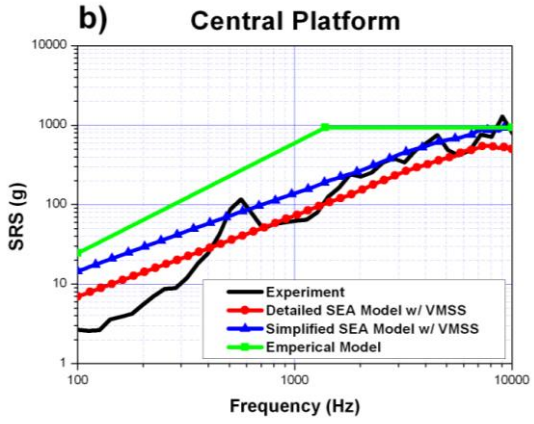

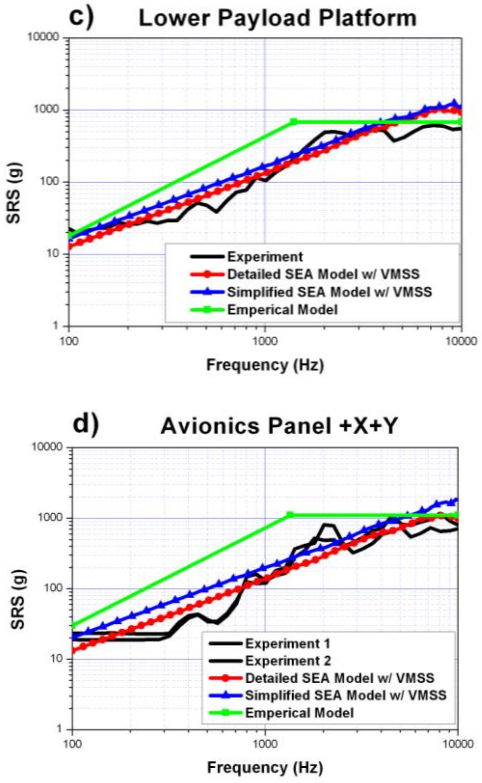

Fig. 6. SRS comparison of launch vehicle separation test results, empirical prediction and SEA with VMSS predictions at a) propulsion platform, b) central platform c) lower payload platform and d) avionics panel +X+Y

For shock predictions using SEA and VMSS, two results, one from the simplified SEA model and the other from the detailed SEA model, are shown. The predicted SRS levels using the detailed SEA model are lower than those resulting from the simplified SEA model near the shock source (avionics panels and central platform), but the prediction results of both the detailed and the simplified SEA models are almost the same at substructures far away from the shock source. This is due to the additional energy dissipation in the detailed SEA model resulting from the inclusion of subsystems omitted in the simplified model. Near the shock source, this additional energy dissipation plays a huge role, but as the shock is transmitted to the upper part of the satellite, shock attenuation due to other factors become dominant. In general, prediction results of the simplified SEA model are better than the detailed model.

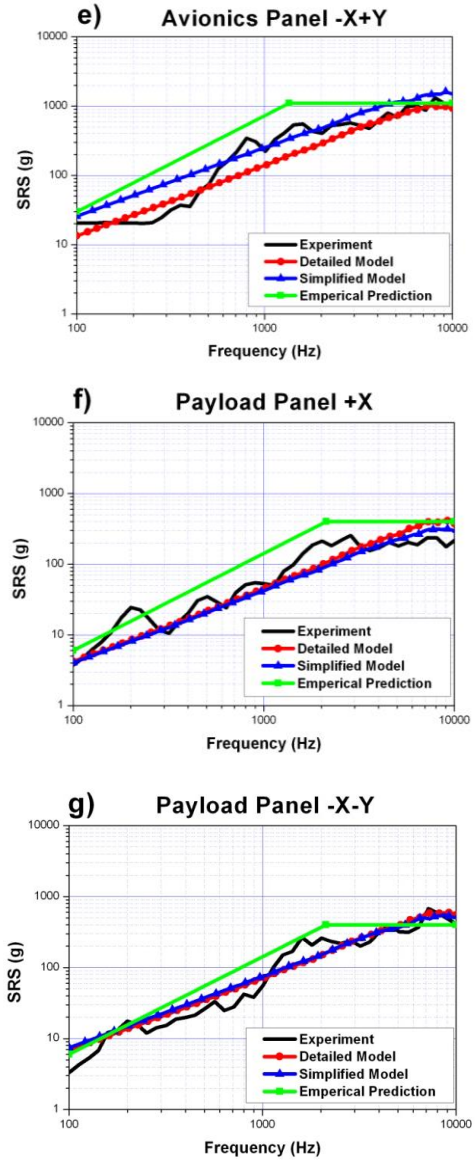

Fig. 6. SRS comparison of launch vehicle separation test results, empirical prediction and SEA with VMSS predictions at e) avionics panel −X+Y, f) payload panel +X and g) payload panel −X−Y

Conclusion

In this paper, shock induced on a low altitude earth observation satellite during launch vehicle separation was predicted using two methods: an empirical model and SEA in conjunction with VMSS. The predictions were then compared and evaluated using test measurements. In general, the predicted shock levels obtained using the empirical model provide

good envelop for the test results in most of the frequency ranges except at very high frequencies. Two SEA models, simplified and detailed, were used with VMSS. The prediction results obtained using the detailed SEA model underestimate SRS level for structures near the shock source. Overall, the SRS predictions given by the simplified SEA model with VMSS are closest to the experimental results.

Acknowledgement

This research has been supported by KOMPSAT-5 System Development Project and Brain Korea (BK) 21.

References

1. Mulville, D.R., 1999, Pyroshock Test Criteria, National Aeronautics and Space Administration.

2. Irvine, T., 2002, An Introduction to the Shock Response Spectrum, Vibrationdata.com.

3. Baumann, R.C., 1996, General Environmental Verification Specification For STS & ELV Payloads, Subsystems, and Components, NASA Goddard Space Flight Center.

4. Himelblau, H. et al., 2001, Dynamic Environmental Criteria, National Aeronautics and Space Administration.

5. Lyon, R.H. and Dejong, R.G., 1998, *Theory and Application of Statistical Energy Analysis* (2nd edition), RH Lyon Corp., Cambridge.

6. Dalton, E., and Chambers, B., 1995, "Analysis and Validation Testing of Impulsive load Response in Complex, Multi-Compartmented Structures", Proceedings of the 36th AIAA Structures, Structural Dynamics, and Materials Conference.

7. VA One 2008 Shock Module User's Guide and Theory, 2008, ESI Group.